Contribution No. 5213 from the Arthur Amos Noyes Laboratory of Chemical Physics, California Institute of Technology, Pasadena, California 91125

Reversible Oxygen Carriers. Synthesis and Structure of μ-Dioxygen-bis[*N*,*N*'-ethylenebis(salicylideniminato)piperidinecobalt] Acetonate Piperidinate, $(C_5H_{11}NCoSalen)_2(O_2)\cdot 0.67(CH_3)_2CO\cdot 0.33C_5H_{11}N_7$

ALEX AVDEEF and WILLIAM P. SCHAEFER*

Received November 18, 1975 AIC50835C

The structure of the title compound has been determined from three-dimensional x-ray data collected by counter methods. The structure has been refined on F^2 using 5314 reflections, including those with negative intensities. The conventional R_F factor based on the portion of the data with F^2 greater than $3\sigma(F^2)$ is 6.9%. The dioxygen adduct of cobalt(II) crystallizes in the orthorhombic space group D_{2h}^{15}-*Pbca* (No. 61), with eight dimers in a cell with the dimensions a = 17.262 (1), b = 19.201 (1), and c = 26.630 (2) Å. The structure consists of dioxygen-bridged dimers of the cobalt Schiff base, with piperidine ligands (chair conformation) completing the octahedral metal coordination. The O–O bond distance, 1.383 (7) Å, suggests a ligand structure which is intermediate between the superoxide and peroxide limits. The Co–O–O–Co torsion angle is 121.9 (4)°. The average values of the coordination bonds are 1.911 (4) Å for Co–O(dioxygen), 1.903 (4) Å for Co–O(Schiff base), 1.875 (14) Å for Co–N(Schiff base), and 2.118 (15) Å for Co–N(piperidine). The lattice contains disordered solvent molecules, acetone and piperidine, which stack loosely in channels parallel to the a axis. Because of the location of the disordered solvent molecules with respect to the positions of the cobalt atoms, the manner in which the weighting scheme is defined and the disorder described has significant bearing on the calculated distances in the dimer. Thermogravimetric analysis shows the crystals to be conditionally stable to 95 °C. At higher temperatures a complicated pattern of weight loss ensues as molecular oxygen along with other material is lost. Upon cooling, oxygen appears to be recaptured by the crystals. The infrared spectrum is reported.

Introduction

Reversibly bound dioxygen adducts of simple transition metal complexes have received considerable attention in the last few years as potential models for the dioxygen-to-metal binding in the complex physiological processes of oxygen transport and storage.[1]

Schiff base complexes of cobalt(II) are well-known oxygen carriers.[2] In the presence of Lewis base, many are able to bind molecular oxygen reversibly to form either dimeric (Co:O_2 = 2:1) dioxygen-bridged species or monomeric (1:1) complexes with dioxygen bonded "end-on". From recent studies of electrochemistry,[3] electron spin resonance,[4] the Lewis base effect and the role of hydrogen bonding,[3-5] and steric hindrance[6,7] properties, the factors influencing the formation of such complexes with both cobalt and iron are partially understood. The structural basis behind reversible dioxygen coordination, on the other hand, has been more difficult to come by due to the inability to grow crystals of adequate quality and stability for x-ray diffraction study. Only a few cobalt Schiff base dioxygen structures are known (1:1,[7b,8,9] 2:1[10-12]). With iron, undoubtedly the most important simple dioxygen adduct to be characterized structurally is the "picket fence porphyrin" complex of Collman and coworkers.[6a]

Some of our own recent efforts have been to synthesize stable substituted CoSalen [CoSalen = *N*,*N*'-ethylenebis(salicylideniminato)cobalt(II)] adducts with the partial aim of obtaining crystals for structural elucidation.[7b,c,10,12] Emphasis as been placed on choosing Lewis bases with (σ + π)-donor properties stronger than that of pyridine. A stable 1:1 complex with *N*-benzylimidazole as the axial ligand has been isolated and its structure determined.[7b] Low-temperature structural work on another related compound having different substituent groups is currently in progress.[7c]

The subject of this paper is the preparation and structure of a 2:1 complex with piperidine as the axial base. The black crystals of the complex are remarkably stable at room temperature. Above 95 °C the crystals turn bright red as molecular oxygen is evolved. Upon cooling, the black color reappears, albeit the material is no longer crystalline. As confirmed by this study the compound is μ-dioxygen-bis-[*N*,*N*'-ethylenebis(salicylideniminato)piperidinecobalt] acetonate piperidinate, $(pipCoSalen)_2(O_2)\cdot 0.67(CH_3)_2CO\cdot 0.33pip$.[13]

Table I. Crystal Data for $(pipCoSalen)_2(O_2)$

Molecular formula:	$(C_5H_{11}NCoN_2O_2C_{16}H_{14})_2(O_2)(C_3H_6O)_{0.67}\cdot(C_5H_{11}N)_{0.33}$
d_{calcd} = 1.384 (1)[a] g/cm³	
Fw 919.92	
Formula units/cell:	8
Linear abs coeff:	μ = 21.1 cm^{-1} (Co Kα radiation)
Crystal dimensions:	nine-sided polyhedron, 0.15 mm along a, 0.11 mm along c, and approximately 0.15 mm along b (0.07–0.22 mm)
Systematic absences:	$0kl, k = 2n + 1; h0l, l = 2n + 1; hk0, h = 2n + 1$
Space group:	D_{2h}^{15}-*Pbca* (No. 61)
Cell parameters (19 ± 1 °C, Co Kα_1, $2\theta_{av} = 90°$).	a = 17.262 (1), b = 19.201 (1), c = 26.630 (2) Å
Cell vol:	V = 8826.5 (11) Å³
F_{000} = 3831.1 e (cor for anomalous dispersion)	

[a] The value appearing in the parentheses here and elsewhere in the report refers to the estimated standard deviation in the least-significant digit.

Experimental Section

Preparation of the Compound. To 50 ml of spectroscopic grade acetone containing approximately $^1/_4$ ml of reagent grade piperidine in a 100-ml volumetric flask 0.20 g of freshly prepared CoSalen·$CHCl_3$[14] was added and the flask was suspended in a cold bath maintained at −15 °C. Pure oxygen was allowed to flow slowly over the surface of the solution for 52 h. Small, well-shaped lustrous black crystals were filtered off. The quality and size of the crystals varied unpredictably from preparation to preparation.

Space Group and Lattice Parameters. The systematic extinctions observed in the reciprocal lattice of *mmm* symmetry are consistent only with the orthorhombic space group *Pbca*. The lattice parameters were obtained from a least-squares fit[15] to angular settings of 13 carefully centered general reflections using Co Kα radiation (λ 1.7902 Å) on a Datex-automated General Electric quarter-circle diffractometer. Assuming a reasonable value for the density, the cell dimensions suggested either sixteen monomers or eight dimers present in the unit cell. The various crystal data are summarized in Table I.

Table II. Results of the Merging of the Duplicated Reflections

	Original[a]					Adjusted[b]				
Octant	R_{F^2}	R_{wF^2}	GOF	Slope[c]	Int[c]	R_{F^2}	R_{wF^2}	GOF	Slope[c]	Int[c]
hkl	0.039	0.055	1.72	1.68	−0.01	0.030	0.052	0.96	1.02	+0.14
$h\bar{k}l$	0.044	0.059	1.87	1.79	−0.49	0.031	0.057	1.03	0.96	−0.23
$\bar{h}kl$	0.046	0.065	1.83	1.74	−0.20	0.037	0.067	1.14	1.02	−0.03
$\bar{h}k\bar{l}$	0.051	0.065	1.81	1.49	+0.99	0.034	0.059	0.96	0.85	+0.17
Mean	0.044	0.060	1.85			0.032	0.058	1.02		

[a] The case with $p = 0.02$ (see text). Agreement factors[23a] are based on deviations from the weighted mean values. [b] Model C with $p = 0.046$ and $F^2(\text{cor}) = [1 + A \sin(\phi + \phi_0)][1 + B \sin(\chi + \chi_0)]F^2(\text{original})$, where $A = 0.061$ (9), $B = -0.091$ (29), $\phi_0 = 46$ (6)°, and $\chi_0 = 25$ (11)°. [c] Slope and intercept (int) refer to the Abrahams-Keve type of plot (see text).

Collection and Reduction of Intensity Data. The crystal was mounted with the $1\bar{2}\bar{1}$ diffraction vector approximately collinear with the ϕ axis of the diffractometer. Over 7000 reflections were measured (using Co Kα radiation, filtered by an iron foil) by the moving-crystal, moving-counter scan technique at a rate of 2° min^{-1} out to $2\theta_{max} = 140°$, using a takeoff angle of 3.5°. Each stationary-background count at the limits of the scan was taken for 20 s.

The intensities of three reflections were monitored approximately once an hour. An average linear decomposition of 1.1%/1000 reflections was observed during the 2-week data collection. Subsequently, the intensities were adjusted for the slight decomposition and were corrected for the usual Lorentz and polarization effects. No absorption corrections were applied, since with $\mu r \approx 0.3$ the errors would amount to about 4% in the extreme cases.

The measured intensities and the associated errors have been defined elsewhere.[12] The Peterson–Levy[16] error factor, p, was assumed to be 2%. There were 5314 unique reflections collected, of which 2554 had $F^2/\sigma(F^2)$ greater than 3.

Solution and Refinement of the Structure. Examination of the Harker sections in a Patterson synthesis map clearly revealed the positions of the two independent cobalt atoms. By applying Fourier syntheses in the usual bootstrap fashion, all of the nonhydrogen atoms were located, including those of a disordered acetone molecule of solvation.

With the model at hand, refinement by full-matrix least-squares using all of the unique reflections including those with negative observed intensities[17] was initiated.[18] After several cycles with isotropic thermal parameters, the hydrogen atoms were included at calculated positions as fixed-atom contributions, assuming C–H and N–H bond distances to be 0.95 Å. Upon converting the thermal parameters of the nonhydrogen and nonsolvent atoms to anisotropic forms, refinement was continued using a three-block matrix.[19]

Unusual Problems with the Disordered Solvent Molecule. After a cycle of anisotropic least squares, it became apparent that the disorder of the acetone molecule was going to be much more of a nuisance than at first anticipated. A scrupulous examination of the electron density map in the region of the solvent molecule suggested two and possibly three orientations for the solvent, with the primary orientation being occupied about 70% of the time. Initial serious attempts to resolve the disorder involved a two-orientation model. Positions and isotropic temperature factors were refined by Fourier difference syntheses, since refinement by least-squares proved unreliable.

In spite of the small residual densities in the region, several strong low-angle reflections were very poorly fitted, much to the detriment of the overall least-squares refinement. The trend in the troublesome reflections suggested that the model could be substantially improved by an increase of electron density in the solvent region. The magnitude of the discrepancies could not be explained by secondary extinction or absorption effects, nor was a three-orientation model a substantial improvement. Since an excess of piperidine was used in the preparation, the partial presence of the base in the solvent region was suspected.[20]

The largest improvement occurred when the solvent region was modified to include partial occupancy by acetone (67%[21]) and piperidine (33%). Probably, additional improvements in the solvent region could be accomplished by making the model more elaborate. The inevitable increase in parameters would in effect lead to an underdetermined problem, since the number of reflections contributing significantly to the large-thermal-parameter solvent region is relatively small.

Error Analysis of the Observed Data. Our problems with the solvent disorder led us to measure some 800 additional reflections covering the region of reciprocal space where the fit was poor. The group consisted of about 200 reflections and their symmetry-related equivalents and served as the basis for error analysis. The agreements between the subsets were evaluated by the method of Abrahams and Keve,[22] where the weighted deviations of reflections from the mean values were plotted against the expected values for a normal distribution with the same sample size. The average slopes of the curves were about 1.7 and thus suggested that our assumed errors were too low or that the deviations were abnormally distributed or a combination of the two. However, the agreement among the subsets was far better than the agreement between F_c and F_o for these reflections, strongly suggesting that our problems in the solvent area were model based rather than data based.

Subsequently, the subsets were merged into the main data set. Naturally, the average weights of the duplicate reflections rose according to the usual expression $w_{av} = \sum w_i$. Later we discovered that this increase in the weights proved to have an unfortunate effect on the structure of the oxygen adduct. Without realizing it at first, we had thus selected our worst-fitted reflections and increased their weights! By this systematic amplification, least-squares refinement of the CoSalen dimer led to a systematically distorted structure, particularly revealing itself in distorted phenyl rings and with unreasonably short Co–N(imine) bond distances. This distorted structure will be referred to as the model A result. Realizing the possible blunder, we remerged the data sets, but this time the weights were averaged arithmetically. The completely converged refinement results of the latter procedure will later be referred to as model B. In both of the above models, $p = 0.02$ (vide supra).

The results of the normal probability analysis were not particularly encouraging. Improvements could result from a change in the p factor or/and adjustments of the observed intensities. A least-squares procedure was evolved to cope with both possibilities, the details of which will be published in a more specialized journal.[23] From the agreement between duplicate reflections obtained from the four different forms, it was possible to deduce a better p factor of 0.046. Also it was possible to adjust intensities for anisotropic systematic errors using a four-parameter function of the variables χ and ϕ, the diffractometer angles. The highest corrections amounted to about 10% and were limited to highly selective regions of the reciprocal space. In the octant in which the main data were collected, the effect of the correction was minimal. The results of the analysis are summarized in Table II. The model which incorporated these improvements is labeled model C and is the most reliable of the three fully refined models.

Table III summarizes the refinement results of the three models examined in detail.

At the end of model C refinement, an agreement analysis of the distribution of errors with respect to the Miller indices and intervals of $(\sin\theta/\lambda, F_o^2$, and $F_o^4/\sigma^2(F_o^2)$ indicated that the agreement between the data and the model was good except for about 60 intense reflections. The *weighted* residuals of these reflections, however, were not much greater than the average for the rest of the data, indicating that our weighting scheme was handling them correctly.

The final parameters for model C are listed in Table IV. The observed and calculated structure factors will appear as supplementary material.[24]

Thermogravimetric Data on the Evolution of Oxygen. The Du Pont 950 thermogravimetric analyzer was used to monitor the weight loss of a 7-mg sample of the crystalline compound as a function of the gradual increase (50 °C min^{-1}) in temperature of helium gas flowing past the sample. The temperature was scanned from 22 to 190 °C, at the end of which the crystals were red. After lowering of the

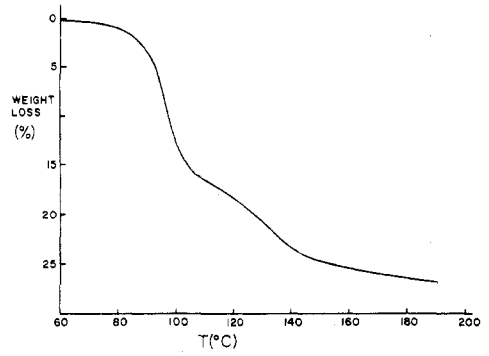

Figure 1. Weight loss of the oxygen adduct as a function of steadily increasing temperature.

temperature back to 22 °C the crystals began to turn black again. In spite of this treatment, the material looked crystalline, with no apparent signs of deterioration. However, there was no longer a diffraction pattern to be observed. The thermogram is presented in Figure 1.

Infrared Measurements. The Perkin-Elmer 225 infrared spectrometer, adapted with a low-temperature cell, was used. At liquid nitrogen temperatures, a KBr pellet or a Nujol mull of the compound appeared stable. However, at the instrument ambient temperature, a pellet begins to turn red after about 30 min. A spectrum[24] was taken at liquid nitrogen temperature.

Results and Discussion

The calculated bond distances and angles along with the atomic labeling scheme are shown in Figure 2 for models A and C. Model B has essentially intermediate values of the three. It was quite surprising that as a result of small changes in the weighting scheme (that is, the p factor mostly contributes to the strong reflections, which are relatively few),

Table III. Summary of the Refinements of Models A, B, and C[a]

	A	B	C
R_F ($F^2 > 3\sigma(F^2)$)	0.088	0.078	0.069
R_{wF} ($F^2 > 3\sigma(F^2)$)			0.074
R_{wF^2} (all data)	0.158	0.167	0.175
GOF (all data)	2.55	1.92	1.34
p	0.02	0.02	0.046
$\Delta\rho$[b] (max)	+1.0[d]	+0.67[d]	+0.57,[e] +0.77[f]
e/Å^3 (min)	−0.7[e]	−0.57[e]	−0.55,[g] −0.54[h]
Δ/σ[c] (max)	2.2 [x of C4(P1), 0.03-Å shift]	0.88 [x of C7(A1), 0.01-Å shift]	0.74 [x of C2(A2), 0.007-Å shift]
	5.2 [β_{11} of C3(P1)]	0.86 [β_{23} of C4(A1)]	1.1 [β_{23} of C3(P1)]

[a] Cf. ref 25b. [b] Residual peak heights from final difference map. [c] Largest shift-over-error in the terminal, anisotropic-mode least-squares refinements. [d] In the vicinity of Co1. [e] In the region between O(A2) and O(B2). [f] Near Co2 and O(A2). [g] Near N(A2). [h] Solvent region.

several bond distances involving the cobalt atoms can change by as much as 0.05 Å. The possibility of similar effects in other published structures containing severe disorder seems real, as well as the possibility of unexpected effects as a result of an arbitrary choice of the p factor. Particular note may be made of the trend in the dioxygen molecule bond length: 1.344 (8) Å[28] for model A, 1.365 (8) Å for model B, and 1.383 (7) Å for model C. The equivalence between these three values can be rejected at the 5% level of significance using the χ^2

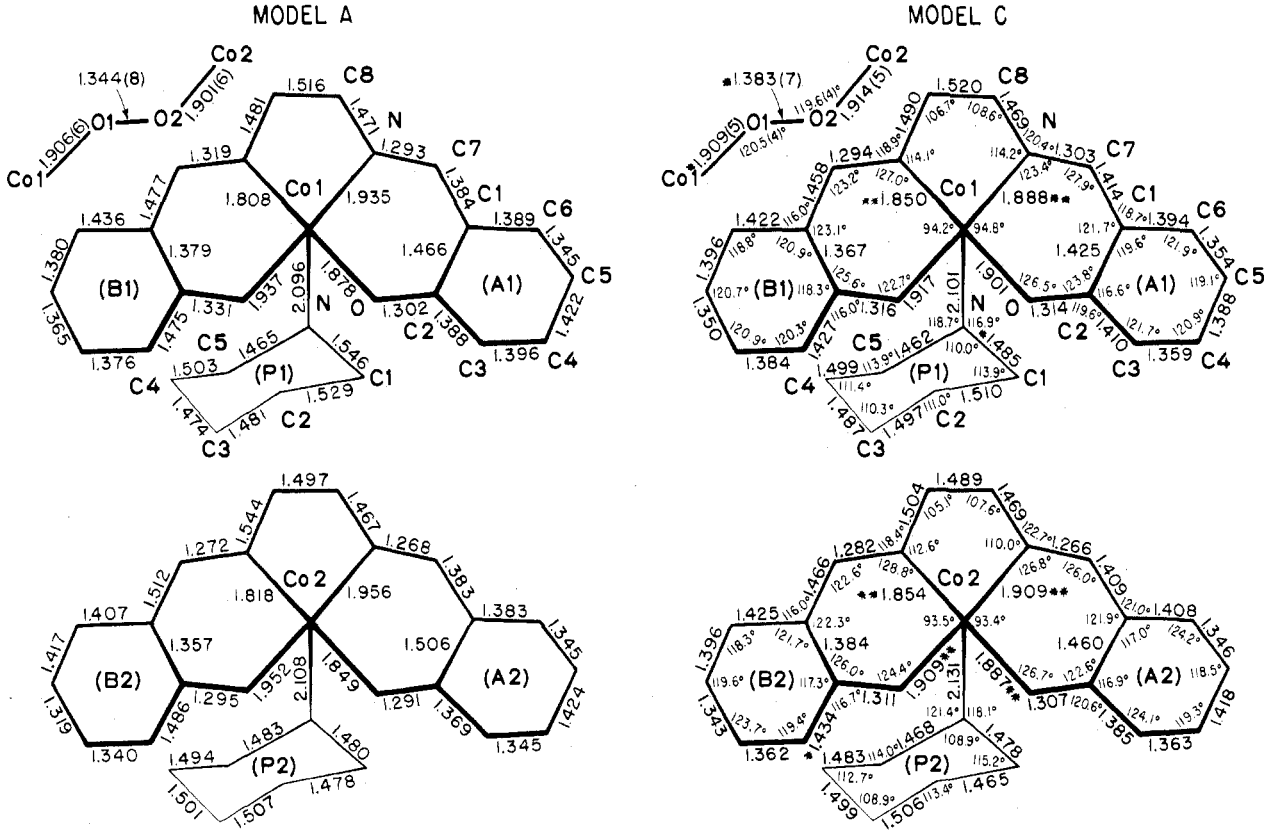

Figure 2. Bond distances, angles, and the labeling scheme in the dimer for models A and C. The various estimated standard deviations[28] in bond lengths and angles are as follows: σ(Co–O) and σ(Co–N), ~0.005–0.006 Å; Salen σ(N–C) and σ(O–C), ~0.009–0.011 Å; Salen σ(C–C), ~0.011–0.015 Å, pip σ(N–C), ~0.011–0.013 Å, pip σ(C–C), ~0.013–0.021 Å, σ(Co-containing angles), ~0.2–0.6°, σ(O–C–C) and σ(N–C–C), ~0.7–0.8°, σ(C–C–C), ~0.7–1.0°. For the meaning of single and double asterisks, see the text.

Table IV. Atomic Parameters[a]

Atom	x	y	z	U_{11}	U_{22}	U_{33}	U_{12}	U_{13}	U_{23}	RMS Amplitudes (Å) 1	2	3
Co1	10757(8)	37981(6)	36531(5)	502(9)	310(7)	481(8)	12(7)	-15(8)	-38(7)	.174	.218	.227
O1	10587(33)	43804(26)	42341(18)	658(41)	332(32)	393(33)	22(31)	-30(33)	-76(26)	.167	.209	.258
O(A1)	-105(32)	36365(25)	36548(22)	536(40)	324(33)	713(43)	-2(29)	-25(35)	21(32)	.180	.231	.268
O(B1)	8254(34)	46331(27)	32937(20)	641(44)	377(34)	502(38)	56(33)	-38(33)	104(30)	.175	.237	.256
N(A1)	13173(39)	29982(30)	40344(24)	562(53)	208(37)	524(46)	80(34)	-26(40)	-31(33)	.138	.226	.244
N(B1)	21342(39)	39425(31)	36204(25)	552(49)	346(40)	487(48)	36(36)	33(41)	-8(36)	.184	.218	.239
N(P1)	10221(45)	33186(35)	29449(25)	792(61)	452(47)	522(49)	134(47)	10(47)	-87(39)	.190	.238	.290
C1(P1)	8626(73)	25589(52)	29362(40)	1455(119)	590(69)	884(86)	322(78)	-199(83)	-172(63)	.214	.288	.405
C2(P1)	6793(93)	22778(63)	24202(50)	2070(169)	940(98)	1048(112)	370(107)	-749(115)	-595(92)	.187	.320	.518
C3(P1)	13008(104)	24659(86)	20526(49)	2773(229)	1751(151)	775(109)	1319(158)	-649(123)	-809(109)	.177	.316	.631
C4(P1)	14329(74)	32309(76)	20542(40)	1424(125)	1770(132)	492(75)	435(106)	62(77)	-230(85)	.207	.343	.456
C5(P1)	16132(64)	34912(51)	25718(35)	965(92)	966(73)	448(62)	31(69)	123(65)	-152(56)	.195	.315	.318
C1(A1)	-126(50)	26980(42)	42593(32)	499(59)	419(55)	575(65)	-109(48)	68(51)	-80(49)	.184	.218	.261
C2(A1)	-3830(50)	31715(47)	39246(33)	424(61)	520(63)	662(66)	32(51)	-6(50)	-84(54)	.203	.221	.265
C3(A1)	-11967(53)	31254(43)	38899(35)	523(67)	415(55)	860(76)	-62(50)	18(57)	-29(52)	.196	.234	.294
C4(A1)	-16117(58)	26887(56)	41880(45)	528(72)	741(81)	1236(104)	-174(64)	118(74)	-147(74)	.207	.277	.362
C5(A1)	-12448(65)	22592(52)	45334(42)	844(93)	607(71)	1031(97)	-218(66)	207(78)	50(65)	.209	.295	.343
C6(A1)	-4612(59)	22529(50)	45533(38)	672(74)	632(71)	867(85)	-136(61)	58(68)	30(62)	.224	.280	.297
C7(A1)	8034(53)	26432(39)	42853(31)	695(68)	256(46)	546(64)	-113(46)	10(54)	68(45)	.146	.237	.269
C8(A1)	21472(52)	29120(43)	41402(35)	508(62)	419(55)	785(76)	167(48)	-14(57)	-43(51)	.170	.251	.282
C1(B1)	20796(54)	51492(46)	33582(33)	541(60)	487(61)	611(68)	-72(53)	99(55)	-40(52)	.208	.224	.266
C2(B1)	13011(58)	51673(43)	32645(29)	747(78)	396(54)	360(51)	37(54)	106(52)	68(45)	.173	.206	.280
C3(B1)	9686(55)	58075(48)	30988(32)	730(74)	596(61)	509(60)	77(59)	91(55)	26(51)	.218	.237	.282
C4(B1)	14281(66)	63922(46)	30370(37)	994(92)	466(61)	689(73)	-20(61)	99(67)	67(53)	.211	.261	.320
C5(B1)	21962(66)	63684(47)	31314(37)	1071(94)	459(64)	749(81)	-153(64)	18(71)	12(57)	.205	.274	.333
C6(B1)	25483(61)	57499(55)	32854(36)	786(75)	668(74)	784(76)	-183(67)	118(66)	-22(66)	.229	.271	.313
C7(B1)	24854(53)	45201(47)	35162(32)	499(63)	569(64)	690(70)	16(52)	65(55)	-44(53)	.217	.238	.268
C8(B1)	26058(53)	33179(45)	37506(34)	606(68)	451(57)	698(67)	127(51)	27(58)	-18(53)	.194	.259	.266
Co2	17185(8)	42386(6)	52144(5)	467(8)	257(7)	437(8)	27(7)	16(8)	-2(6)	.159	.208	.218
O2	9506(31)	40964(24)	47061(18)	594(39)	339(30)	388(33)	14(28)	28(30)	-7(25)	.183	.197	.245
O(A2)	26356(30)	41111(23)	48401(19)	500(37)	203(27)	571(38)	-5(26)	90(32)	35(27)	.141	.210	.252
O(B2)	17392(32)	32594(23)	53379(19)	533(37)	232(28)	670(41)	5(29)	83(35)	52(27)	.150	.222	.267
N(A2)	16631(41)	52101(29)	50654(23)	611(51)	237(36)	538(47)	30(37)	-40(42)	19(32)	.152	.229	.251
N(B2)	8617(40)	43833(33)	56209(24)	570(52)	381(43)	460(46)	-4(37)	62(40)	15(36)	.194	.209	.245
N(P2)	24871(39)	43174(33)	58381(24)	530(46)	393(40)	550(47)	-26(37)	-71(42)	2(37)	.197	.230	.235
C1(P2)	22384(62)	40136(48)	63220(33)	1065(92)	769(72)	420(56)	-435(65)	-191(60)	171(53)	.187	.218	.380
C2(P2)	28556(67)	39179(57)	66931(35)	1237(103)	1068(88)	589(69)	-494(79)	-447(69)	328(63)	.187	.256	.435
C3(P2)	33202(69)	45680(63)	67890(37)	1103(96)	1238(100)	542(69)	-289(86)	-470(70)	112(67)	.165	.315	.402
C4(P2)	35764(61)	48654(51)	62955(35)	1073(91)	811(73)	562(63)	-363(66)	-380(65)	81(58)	.181	.254	.384
C5(P2)	29266(61)	49575(48)	59370(34)	982(85)	560(64)	608(66)	-211(61)	-279(62)	60(53)	.206	.228	.347
C1(A2)	28703(50)	53260(41)	46383(31)	544(58)	336(50)	590(64)	-63(47)	-29(50)	-77(45)	.171	.237	.248
C2(A2)	31047(47)	45979(40)	46813(27)	550(62)	368(50)	304(49)	68(45)	37(43)	-59(38)	.159	.200	.226
C3(A2)	38582(53)	44380(41)	45445(31)	562(63)	487(53)	599(61)	6(50)	114(55)	74(47)	.206	.226	.267
C4(A2)	43761(55)	49115(49)	43640(38)	599(70)	634(66)	1000(86)	-121(56)	244(64)	9(62)	.205	.263	.335
C5(A2)	41437(58)	56154(51)	43057(39)	696(73)	544(70)	1163(92)	-304(59)	286(68)	100(64)	.153	.295	.361
C6(A2)	34191(55)	57942(41)	44406(35)	772(75)	322(48)	802(70)	-128(55)	91(61)	26(50)	.168	.269	.298
C7(A2)	21473(52)	55628(36)	48149(31)	744(67)	177(42)	491(55)	-111(42)	-55(53)	1(40)	.125	.219	.279
C8(A2)	9082(50)	54891(42)	52216(33)	577(64)	427(53)	649(64)	304(47)	-17(56)	-50(49)	.137	.253	.288
C1(B2)	5027(52)	31817(46)	57470(29)	579(62)	578(62)	399(53)	-25(54)	136(49)	71(48)	.175	.244	.256
C2(B2)	11615(50)	29040(40)	55290(30)	512(59)	382(49)	501(58)	-44(46)	-65(52)	14(43)	.192	.211	.241
C3(B2)	12361(51)	21604(43)	55279(33)	610(67)	423(55)	654(65)	-125(48)	0(54)	75(48)	.186	.253	.265
C4(B2)	6721(60)	17648(46)	57433(37)	770(78)	466(61)	918(81)	-128(57)	-113(66)	94(58)	.203	.269	.319
C5(B2)	277(61)	20296(51)	59519(38)	861(84)	617(68)	843(81)	-385(64)	-46(68)	199(61)	.173	.284	.348
C6(B2)	-838(53)	27494(53)	59581(33)	560(66)	848(77)	575(63)	-170(59)	96(53)	-21(57)	.209	.247	.306
C7(B2)	3818(50)	33345(47)	57951(32)	489(62)	628(63)	549(60)	169(50)	21(50)	-51(50)	.191	.236	.273
C8(B2)	6930(51)	51432(43)	57024(33)	569(64)	436(56)	681(67)	92(48)	-16(53)	-177(50)	.179	.240	.281

Acetone

Atoms	x	y	z	B (Å^2)
O'	4013	3691	2723	12.3
C1'	3668	4635	2207	10.8
C2'	4154	4316	2612	7.2
C3'	4794	4695	2893	6.8

Piperidine Solvent

Atoms	x	y	z	B (Å)
N''	4693	4306	3045	10.8
C1''	4160	3646	3123	12.2
C2''	3914	3451	2543	10.9
C3''	3827	4065	2334	11.6
C4''	4080	4928	2432	12.2
C5''	4565	5054	2838	12.2

Hydrogen	At	x	y	z	Hydrogen	At	x	y	z	Hydrogen	At	x	y	z
H1	C8(A1)	2290	2440	4133	H24	C3(B2)	1677	1939	5371	H47	C4(P2)	3955	4558	6151
H2	C8(A1)	2261	3100	4469	H25	C4(B2)	732	1279	5749	H48	C4(P2)	3810	5304	6352
H3	C8(B1)	3088	3459	3887	H26	C5(B2)	-345	1724	6096	H49	C5(P2)	2588	5286	6069
H4	C8(B1)	2685	3035	3466	H27	C6(B2)	-540	2950	6106	H50	C5(P2)	3140	5107	5627
H5	C8(A2)	526	5374	4972	H28	C7(B2)	-54	4119	5966	H51	C1'	3213	4337	2150
H6	C8(A2)	924	5976	5263	H29	N(P1)	569	3565	2841	H52	C1'	3925	4553	1878
H7	C8(B2)	990	5335	5969	H30	C1(P1)	444	2457	3154	H53	C1'	3569	5075	2274
H8	C8(B2)	155	5214	5771	H31	C1(P1)	1315	2317	3051	H54	C3'	4558	5017	3127
H9	C3(A1)	-1455	3401	3647	H32	C2(P1)	191	2477	2310	H55	C3'	4965	5112	2674
H10	C4(A1)	-2162	2676	4162	H33	C2(P1)	616	1786	2433	H56	C3'	5113	4390	3040
H11	C5(A1)	-1535	1983	4757	H34	C3(P1)	1131	2324	1728	H57	C1''	3704	3759	3327
H12	C6(A1)	-210	1951	4781	H35	C3(P1)	1748	2223	2145	H58	C1''	4447	3264	3281
H13	C7(A1)	986	2312	4522	H36	C4(P1)	999	3466	1930	H59	C2''	3429	3186	2535
H14	C3(B1)	425	5837	3033	H37	C4(P1)	1874	3323	1844	H60	C2''	4323	3184	2376
H15	C4(B1)	1207	6820	2923	H38	C5(P1)	2090	3285	2684	H61	C3''	3261	4098	2313
H16	C5(B1)	2501	6776	3096	H39	C5(P1)	1673	3981	2562	H62	C3''	4042	3982	1999
H17	C6(B1)	3101	5737	3343	H40	N(P2)	2829	4004	5669	H63	C4''	3602	5194	2484
H18	C7(B1)	3038	4528	3541	H41	C1(P2)	2002	3584	6260	H64	C4''	4342	5096	2129
H19	C3(A2)	4018	3969	4577	H42	C1(P2)	1864	4332	6461	H65	C5''	4315	5354	3088
H20	C4(A2)	4887	4761	4276	H43	C2(P2)	3186	3566	6577	H66	C5''	5054	5266	2731
H21	C5(A2)	4492	5952	4173	H44	C2(P2)	2618	3781	7001	H67	N''	5229	4225	3152
H22	C6(A2)	3273	6263	4399	H45	C3(P2)	3761	4447	6987					
H23	C7(A2)	2021	6028	4730	H46	C3(P2)	3015	4897	6963					

[a] The x, y, z fractional coordinates are multiplied by 10^5 in the case of the non-solvent, non-hydrogen atoms and by 10^4 otherwise. The form of the thermal ellipsoid is $\exp[-2\pi^2(U_{11}h^2a^{*2}+U_{22}k^2b^{*2}+U_{33}\ell^2c^{*2}+2U_{12}hka^*b^*+2U_{13}h\ell a^*c^*+2U_{23}k\ell b^*c^*)]$. The U_{ij} elements in the table are multiplied by 10^4. B = 6 Å^2 for H1 through H50; B = 10 Å^2 for H51 through H56; and B = 12 Å^2 for the remaining hydrogens.

Table V. Comparison of 2:1 Dioxygen Adducts

Complex	O-O, Å	Co-O-O, deg	Co-O, Å	Co(O)(O)Co, deg[a]	Co···Co, Å	Ref
$K_5[Co_2O_2(CN)_{10}]\cdot H_2O$	1.243 (13)	121.2	1.944	166	4.637	30
	1.289 (20)	120.7	1.919	180	4.634	
$K_8[Co_2O_2(CN)_{10}](NO_3)_2\cdot 4H_2O$	1.447 (4)	118.8	1.985	180	4.899	31
$[Co_2O_2(NH_3)_{10}](NO_3)_5$	1.317 (20)	117.3	1.895	180	4.545	32
$[Co_2O_2(NH_3)_{10}](SO_4)(HSO_4)_3$	1.312 (20)	117.7	1.894	175.3	4.562	33
$[Co_2O_2(NH_3)_{10}](SO_4)_2\cdot 4H_2O$	1.473 (10)	113	1.883	145.8	4.427	34
$[Co_2O_2(NH_3)_{10}](SCN)_4$	1.469 (6)	110.8	1.879	180	4.495	35
$[Co_2O_2(en)_2(dien)_2](ClO_4)_4$[b]	1.488 (6)	110.0	1.896	180	4.523	36
$[Co_2O_2(en)_2(NO_2)_2](NO_3)_2\cdot 4H_2O$	1.53	110	1.89	180	4.54	37
$[Co_2O_2(NH_2)(en)_4](NO_3)_4$[c]$\cdot H_2O$	1.353	119.2	1.878	23.4	3.276	38
$[Co_2(O_2H)(NH_2)(en)_4](NO_3)_4$[d]$\cdot 2H_2O$	1.42	115	1.92		2.98	38
$[Co_2O_2(NH_2)(NH_3)_5](NO_3)_4$[c]	1.320 (5)	120.9	1.867	0.0	3.242	39
$(CoSalen)_4(O_2)_2(H_2O)_2\cdot pip\cdot 2CHCl_3$	1.308 (28)	118	1.931, 2.000	122		10
$(CoSalen)_2(O_2)(DMF)_2$[e]	1.339 (6)	120.3	1.910	110.1		11
$Co_2(Salprtr)_2(O_2)\cdot$(toluene)[f]	1.45 (2)	118.5	1.93	149.3	4.65	12
$(CoSalen)_2(O_2)]\cdot {}^2/_3(CH_3)_2CO\cdot {}^1/_3pip$	1.383 (7)	120.0	1.911	121.9	4.386	This work

[a] Torsion angle. [b] en = ethylenediamine; trien = diethylenetriamine. [c] Bridging dioxygen and amide groups. [d] Bridging hydroperoxo and amide species. [e] DMF = dimethylformamide. [f] Salprtr = 3,3'-diiminodi-*n*-propylaminebis(salicylaldehyde).

test.[29] Similar variations are noted in other bonds (denoted by an asterisk in Figure 2). The changes in the cobalt–imine nitrogen distances are even more significant, where equivalence can be ruled out at the 1% level (double asterisk in Figure 2). Thus, in numerous important aspects, model C is significantly different from the other two models; our results here are based on model C.

The problems caused by the disordered solvent are real and the effect is such that the estimated standard deviations in the calculated bond distances and angles reported here (as obtained from the last cycle of least-squares refinement) should be increased before any chemical comparisons are made. Table VII gives the esd's for some of the groups of distances in this structure, with esd's for the group considering the bonds chemically equivalent, and individual bond length esd's. The ratio of these numbers varies from 2 to 4.7, indicating that all of our individual esd's should be multiplied by 3 or so to reflect the true precision of the determination. This procedure should be standard in structures where the model does not fit the data well. A structure is not necessarily incorrect or useless if it contains disordered regions, but neither is a structure correct (nor its esd's accurate) just because a least-squares refinement has converged. Any structure which shows chemically unreasonable bond distances or angles must be viewed with suspicion, but, if the data are good, even a structure with significant disorder can be refined, with care, to give useful results.

Dioxygen Coordination. The O1–O2 bond length, 1.383 (7) Å, is between the usually quoted[27] values of 1.28 Å for the superoxide (O_2^-) and 1.49 Å for the peroxide (O_2^{2-}) species. The range of the observed values for complexes containing these ligands is actually quite large, as shown in Table V, and is consistent with a delocalized molecular orbital view of the bonding of the dioxygen ligand to the metal complex. The bond length in the present case is somewhat longer than that found in the comparable Co(3-FSalen) tetrameric oxygen adduct[10] and the DMF (dimethylformamide) dimeric CoSalen oxygen adduct.[11] The latter complex is thought[11] to possess an unusual electronic structure due to its relatively short O_2 bond in light of its nonplanar Co–O–O–Co group and its diamagnetic state.

Of the structural parameters listed in Table V, only the Co–O–O angles appear to correlate with the O–O bond distances, as shown in Figure 3. Although the fit is not exceptionally good, it does appear to suggest that with superoxide adducts the oxygen atoms are more nearly sp^2 hybridized and with peroxide adducts they are more nearly tetrahedrally (sp^3) hybridized. In additon, the angles are nearly uniformly distributed throughout the range, again suggesting valence delocalization.

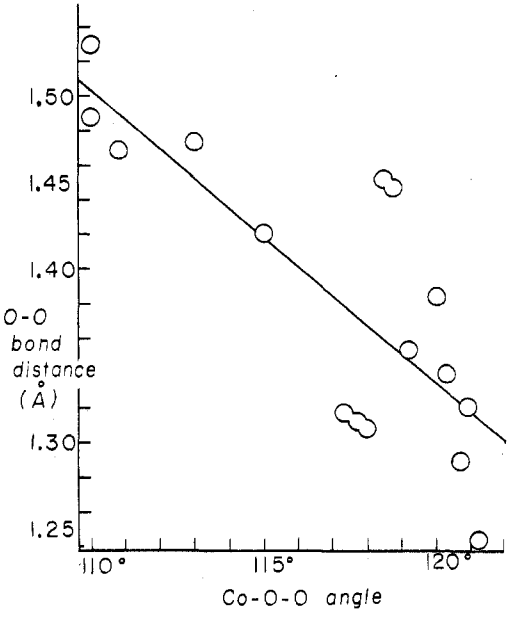

Figure 3. Plot of the O-O bond distances vs. the Co-O-O angles in 2:1 oxygen adduct complexes.

The Co–O–O–Co torsion angles in the 2:1 complexes assume a wide range of values and appear to obscure any systematic trends with respect to other geometrical parameters. The angle in the present compound, 121.9 (4)°, seems to be typical of the bulky Schiff base adducts and in such compounds may indeed be constrained to a narrow range of possible values due to unfavorable contacts between the halves of the dimer. A simple description of the O_2 coordination would predict an exactly planar Co–O–O–Co unit only in the case of a formally neutral singlet electronic state O_2 species. None of the 2:1 complexes have dioxygen bond distances so short as to suggest such a case.

Due to the symmetrical arrangement of the nonpolar dioxygen ligand in the 2:1 adducts, the facile identification of the O_2 stretching vibration in the infrared spectrum is not possible. The spectrum of the dimer[24] is similar to that reported by Floriani and Calderazzo.[40] Of primary concern to

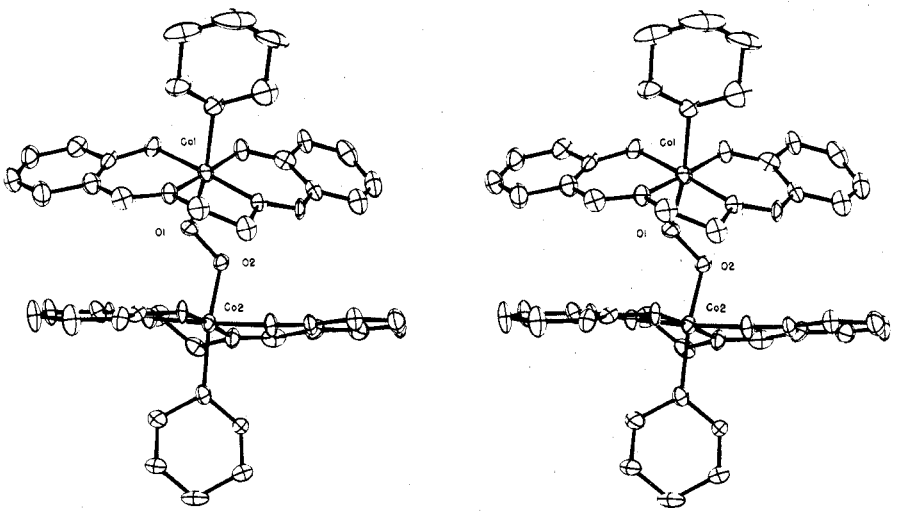

Figure 4. ORTEP-drawn[15] stereoview of the dimer. The upper CoSalen A1 residue (cf. Figure 3) is on the right side of the drawing, while the A2 portion of the lower CoSalen is on the left side.

Table VI. Deviations (in 10^{-2} Å Units) from Mean Planes[a]

	M1[b]	A1	B1		M2	A2	B2
Co1	0*	23	38	Co2	0*	−29	26
O1	190	213	215	O2	189	149	208
O(A1)	−3*	5*	65	O(A2)	−5*	6*	41
N	5*	−5*	87	N	6*	−13*	62
C1	41	4*	171	C1	−24	9*	65
C2	16	0*	122	C2	−32	1*	39
C3	13	−11*	137	C3	−71	−11*	11
C4	42	−7*	203	C4	−98	−13*	10
C5	74	5*	257	C5	−86	−1*	40
C6	69	6*	237	C6	−50	9*	65
C7	33	0*	149	C7	1	7*	80
C8	11	2	83	C8	37	−9	84
O(B1)	4*	60	−2*	O(B2)	4*	−35	0*
N	−5*	32	4*	N	−9*	−75	−1*
C1	55	135	0*	C1	39	−52	3*
C2	45	121	2*	C2	31	−35	3*
C3	74	172	3*	C3	48	−21	0*
C4	113	233	2*	C4	70	−26	−4*
C5	123	247	0*	C5	79	−41	−2*
C6	93	197	−3*	C6	65	−54	2*
C7	25	85	−5*	C7	16	−75	−2*
C8	−43	−24	−10	C8	−34	−103	−10
$\bar{d}$	2	6	3		2	9	2
h[c]	−1.122	−0.259	−3.176		−9.753	−6.560	−8.044
k	9.889	12.845	5.031		−3.283	−2.535	−0.422
l	22.769	19.786	25.245		−21.490	−24.393	−23.568
D	11.951	11.853	10.399		−14.277	−14.268	−14.111

[a] The atoms used for fitting are denoted by asterisks beside their deviations. The weights used, $1/\sigma_i^2$, were derived from the isotropic coordinate errors σ_i. The root-mean-square deviations (in units of 10^{-2} Å) are denoted by $\bar{d}$. [b] M1 and M2 are called "basal" planes, while A1, A2, B1, and B2 are called "wing" planes in the text. [c] The form of the equation defining the plane is $hx + ky + lz = D$, where x, y, and z are the fractional coordinates.

us, the spectrum did not support the highly distorted model A structure of the dimer and was thus instrumental in instigating further examination.

Salen Ligands. The average Co–O(dioxygen) and Co–O(phenolic) bond lengths, 1.911 [4, 3][42] and 1.903 [2, 4] Å, respectively, are typical of the majority of the known 2:1 adducts (see ref 41 and Table V). The average Co–N(imine) distance, 1.875 [3, 14] Å, is slightly shorter than expected in six-coordinate CoSalen complexes,[41] although the difference is well within range of the present experimental errors.

As can be seen in Figure 4 and more clearly in Figure 5, both the "umbrella" and the "step" distortions[41] are present in the dimer. Neither type is unusual in five- and six-coordinate MSalen compounds.[41] The least-squares planes analysis, Table VI, shows each CoSalen residue to possess three distinct planes: one "basal" and two "wings" (cf. Table VI). The dihedral angles between the wing and the basal planes (shown in Figure 5) characterize the degree of umbrella or step distortion.

Table VII compares the dimensions of the Salen portion with related structures. The average Salen ligand dimensions of the oxygen adducts are indistinguishable from those of other six-coordinate CoSalen compounds. The coordination bonds in four-coordinate compounds are shorter than those found in the oxygen adducts, which is consistent with the expected increase in the crystal field repulsion in going from fourfold to sixfold coordination.

The ethylenediamine torsion angles, N(imine)–C8–C8'–N(imine)', are 33.2 (9) and 45.5 (8)° in the A1–B1 and A2–B2 fragments.

Table VII. Dimensions (Å) of 2:1 Oxygen Adducts and Related Cobalt-Schiff Base Complexes[a]

	Co–O[b]	Co–N[d]	O–C2	N–C7	C7–C1	C1–C2	C2–C3	C3–C4	C4–C5	C5–C6	C6–C1	Ref
Av dimensions of four four-coordinate CoSalen compounds	1.851	1.859	1.312	1.290	1.434	1.416	1.420	1.375	1.402	1.366	1.416	7, 41
Av dimensions of six six-coordinate CoSalen compounds	1.906	1.887	1.311	1.291	1.429	1.422	1.417	1.387	1.404	1.365	1.421	41
$(CoSalen)_4(O_2)_2(H_2O)_2 \cdot 2CHCl_3 \cdot pip$	1.916	1.889	1.331	1.282	1.403	1.447	1.416	1.360	1.433	1.400	1.407	10
$(DMF)CoSalen)_2(O_2)$	1.902	1.883	1.318	1.292	1.426	1.429	1.410	1.401	1.393	1.364	1.431	11
$(CoSalprtr)_2(O_2)$[e]	1.90	1.94	1.33	1.27	1.42	1.40	1.42	1.42	1.35	1.33	1.45	12
$(pipCoSalen)_2(O_2) \cdot {}^1/_3pip \cdot {}^2/_3(CH_3)_2CO$[f]	1.903 [2, 4]**	1.875 [3, 14]**	1.312 [5, 6]	1.286 [5, 8]	1.435 [6, 11]*	1.410 [6, 22]**	1.414 [6, 12]**	1.367 [6, 8]	1.376 [7, 15]**	1.373 [7, 15]**	1.413 [6, 9]	This work
Av dimensions of oxygen adducts	1.907	1.892	1.322	1.283	1.420	1.424	1.415	1.379	1.394	1.373	1.420	

[a] Labeling scheme is the same as in Figure 3 for the CoSalen portion. [b] Phenolic oxygen. [c] Salprtr is defined in Table V. [d] Imine nitrogen. [e] See ref 42. [f] Single asterisk signifies nonequivalent bonds at the 5% level of significance,[29] while double asterisks correspond to nonequivalence at the 1% level.

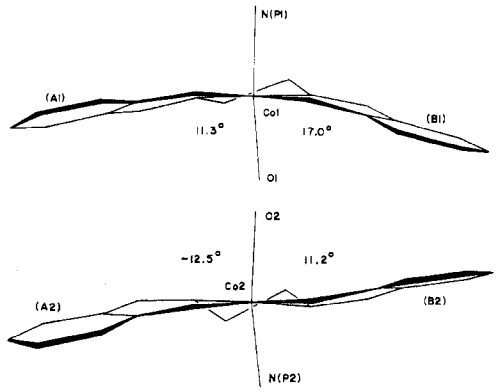

Figure 5. View normal to the best plane through the Salen oxygen and nitrogen atoms in the halves of the dimer. The dihedral angles between the "wings" and the "base" (see text) are shown.

Table VIII. Selected Intra- and Intermolecular Contact Distances and Angles[a]

Co1···Co2 = 4.386 (2) Å

Contacts under 3.4 Å

C8(A1)···O(A2)	3.08 (1)	C8(B1)···O(A2)	3.28 (1)
C8(B2)···O(A1)^{I}	3.13 (2)	C8(A1)···O(B2)	3.33 (1)
C8(B2)···O1^{I}	3.16 (2)	O2···C8(A2)^{I}	3.31 (2)
C7(B1)···C2(A2)	3.28 (1)	O2···C8(B2)^{I}	3.37 (2)

Hydrogen Contacts under 2.5 Å
(Assuming Bonding Distances C–H and N–H as 0.95 Å)

O1···H8^{I}	2.24	O(A1)···H29	2.38
O(A2)···H40	2.24	O(B1)···H29	2.42

Solvent Contacts under 3.6 Å

C(1″)···C7(B1)	3.50	C(1″)···C5(B2)^{III}	3.16
C(1″)···C8(B1)	3.23	C(3″)···O(A1)^{II}	3.41

Angles, Deg

O2–O1···H8^{I}	91	N(P1)–H29···O(B1)	97
Co1–O1···H8^{I}	102	N(P1)–H29···O(A1)	96
O1···H8^{I}–C8(B2)	162	N(P2)–H40···O(B2)	93

[a] Roman numeral superscripts refer to equivalent positions relative to the reference molecule at x, y, z: (I) $-x, 1-y, 1-z$; (II) $x-{}^1/_2, y, {}^1/_2-z$; (III) $x+{}^1/_2, {}^1/_2-y, 1-z$.

Piperidine Ligands. Both of the piperidine ligands are in the chair conformation. The torsion angles N–C1–C2–C3 and N–C5–C4–C3 are 53.7 (14) and −56.0 (13)°, respectively, in molecule P1 and 52.6 (12) and −56.0 (11)°, respectively, in molecule P2 (Figure 2).

The particular orientation of the piperidine molecules relative to the atoms in the basal planes (vide supra) may indicate the presence of weak hydrogen bonding N(pip)–H···O(phenolic), where the shortest H···O distances are 2.2 and 2.4 Å in molecules P1 and P2, respectively (Table VIII).

The Co–N(pip) average distance, 2.118 [5, 15] Å,[42] is slightly long for what is expected for a Co^{III}–N bond but is consistent with the steric requirements[3] of the secondary amine. The average piperidine bond lengths N–C1 (1.473 [6, 7] Å), C1–C2 (1.486 [7, 10] Å), and C2–C3 (1.499 [9, 5] Å) are considerably shorter than expected,[44,45] a result which is attributable to excessive thermal motion (Table IV). Although one usually does not view piperidine molecules as rigid bodies, it is nonetheless moderately instructive to examine the results of a Schomaker–Trueblood[46] type of thermal motion analysis. In piperidine P1, the largest motion is a wagging of rms amplitude 10° about an axis inclined about 30° to the Co(1)–N(P1) axis. There is a moderate screw component coupled to this wagging. Piperidine P2 has a smaller (4° rms) libration approximately about the Co(2)–N(P2) axis, again coupled with a moderate screw component. Neither ligand is described particularly well as a rigid body. The average piperidine bond

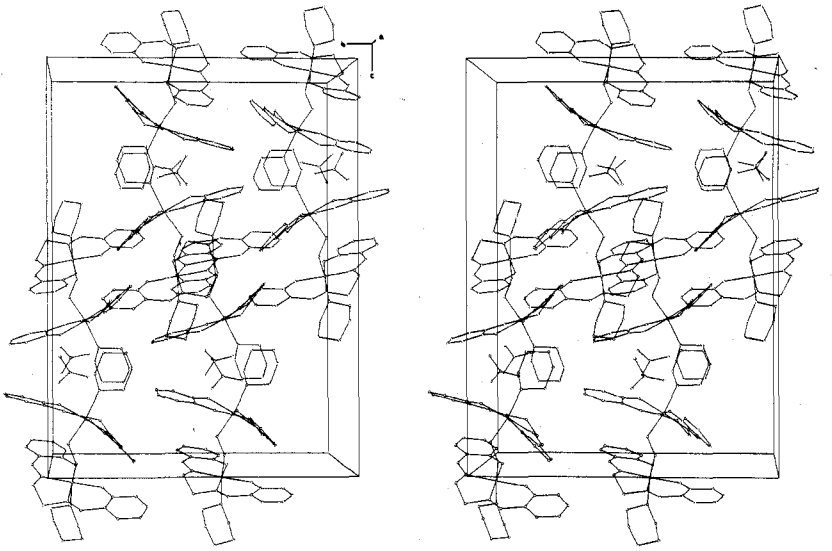

Figure 6. View of the cell packing. The piperidine solvent molecules have been excluded for clarity. The Salen ligands more nearly perpendicular to the view are associated with Co1.

lengths corrected for the thermal motion are in better agreement with previous observations (N–C1 = 1.48 Å, C1–C2 = 1.49 Å, and C2–C3 = 1.51 Å).

Nonbonded Contact Distances and Packing Considerations. Table VIII lists some of the shorter nonbonding contact distances and angles. Of particular interest are the hydrogen contacts. The ethylenediamine hydrogen, H8, in one dimer is 2.2 Å from one of the oxygen atoms in the dioxygen ligand in another inversion-related dimer. This =N–C–H···O interaction is sometimes called a weak hydrogen bond,[47] since the H···O distance is about 0.4 Å shorter than the sum of the van der Waals radii.

Figure 6, showing the molecular packing in the cell, reveals the linear stacking, parallel to the *a* axis, of the acetone molecules and also the piperidine ligands associated with Co1. The region of these channels exhibits loose packing, characterized by large thermal motions (vide supra) and large intermolecular separations, an arrangement which could facilitate the loss of the solvent and half of the coordinated piperidine molecules, consistent with the thermal degradation[48] shown in Figure 1.

Conclusion

In spite of difficulties in the interpretation of the diffraction data, an accurate assessment of the geometry of the dioxygen adduct is possible when one considers the mean values of the four chemically equivalent residues of the dimer (Table VII). The bond length in the dioxygen ligand is unusual by comparison to other known structures in that it is too long to suggest an O_2^- species, yet too short for O_2^{2-}. We have taken this to mean that perhaps there are no "correct" superoxide or peroxide bond lengths. That is, the coordination is valence delocalized and the O_2 bond length can assume any value within a wide range, depending on numerous electronic factors. The observed length, however, probably relates to the degree of reversibility of the dioxygen coordination. Although we have not observed a truly reversible behavior, since more than oxygen comes off upon heating, the reappearance of the black color in the crystals does suggest the reincorporation of O_2, based on previous studies.[2] Similar behavior is not observed in complexes with O_2 bond length greater than ~1.4 Å. The lack of discernible differences in the Salen ligands between oxygen adducts and other six-coordinate CoSalen compounds possibly suggests that the Lewis bases completing the six-coordination in oxygen adducts have the final role in "fine tuning" the reversibility in the dioxygen coordination.

Acknowledgment. We wish to thank R. E. Marsh for his continued interest in our work and for the many insightful discussions on the subject of this paper. We thank Sten Samson for his construction and maintenance of the x-ray equipment. This work was partially supported by the National Institute of Health under Grant No. HL-12395 from the National Heart and Lung Institute.

Registry No. $[(pipCoSalen)_2(O_2)]\cdot{}^2/_3(CH_3)_2CO\cdot{}^1/_3pip$, 58512-27-9.

Supplementary Material Available: Listing of structure factor amplitudes and an ir spectrum (22 pages). Ordering information is given on any current masthead page.

References and Notes

(1) (a) M. N. Hughes, "The Inorganic Chemistry of Biological Processes", Wiley, New York, N.Y., 1972, Chapter 7; (b) J. S. Valentine, *Chem. Rev.*, **73**, 235 (1973); (c) G. Henrici-Olivé and S. Olivé, *Angew. Chem., Int. Ed. Engl.*, **13**, 29 (1974).

(2) (a) T. Tsumaki, *Bull. Chem. Soc. Jpn.*, **13**, 252 (1938); (b) E. W. Hughes, W. K. Wilmarth, and M. Calvin, *J. Am. Chem. Soc.*, **68**, 2273 (1946), and references therein.

(3) (a) G. Costa, G. Mestroni, A. Puxeddu, and E. Reisenhofer, *J. Am. Chem. Soc.*, **92**, 2870 (1970); (b) M. J. Carter, D. P. Rillema, and F. Basolo, *ibid.*, **92**, 61 (1970); **96**, 392 (1974).

(4) (a) H. Kon and N. E. Sharpless, *Spectrosc. Lett.*, **1**, 49 (1968); (b) E. Earnshaw, P. C. Hewlett, E. A. King, and L. F. Larkworthy, *J. Chem. Soc. A*, 241 (1968); (c) B. M. Hoffman, D. I. Diemente, and F. Basolo, *J. Am. Chem. Soc.*, **92**, 61 (1970); (d) B. M. Hoffman and D. H. Petering, *Proc. Natl. Acad. Sci. U.S.A.*, **67**, 637 (1970); (e) J. C. W. Chien and L. C. Dickinson, *ibid.*, **69**, 2783 (1972); (f) F. A. Walker, *J. Am. Chem. Soc.*, **92**, 4235 (1970); **95**, 1154 (1973); (g) H. C. Stynes and J. A. Ibers, *ibid.*, **94**, 1559 (1972); (h) E. Melamud, B. L. Silver, and Z. Dori, *ibid.*, **96**, 4689 (1974); (i) B. B. Wayland, J. V. Minkiewicz, and M. E. Abd-Elmageed, *ibid.*, **96**, 2795 (1974).

(5) (a) A. L. Crumbliss and F. Basolo, *J. Am. Chem. Soc.*, **92**, 55 (1970); (b) J. P. Collman, H. Takaya, B. Winkler, L. Libit, S. S. Koon, G. A. Rodley, and W. T. Robinson, *ibid.*, **95**, 1656 (1973); (c) C. K. Chang and T. G. Traylor, *ibid.*, **95**, 5810 (1973); (d) D. V. Stynes, H. C. Stynes, J. A. Ibers, and B. R. James, *ibid.*, **95**, 1142 (1973); (e) W. S. Caughey, *Adv. Chem. Ser.*, **No 100**, Chapter 12 (1971).

(6) (a) J. P. Collman, R. R. Gagne, C. A. Reed, W. T. Robinson, and G. A. Rodley, *Proc. Natl. Acad. Sci. U.S.A.*, **71**, 1326 (1974); (b) J. P. Collman, R. R. Gagne, and C. A. Reed, *J. Am. Chem. Soc.*, **96**, 2629 (1974); (c) J. E. Baldwin and J. Huff, *ibid.*, **95**, 5758 (1973); (d) J. Almog, J. E. Baldwin, and J. Huff, *ibid.*, **97**, 227 (1975).

(7) (a) G. G. Christoph, J. F. Rogers, and W. P. Schaefer, Paper D1, American Crystallographic Association Winter Meeting, Gainesville, Fla., Jan 1973; (b) R. S. Gall, J. R. Rogers, W. P. Schaefer, and G. G. Christoph, *J. Am. Chem. Soc.*, in press; (c) A. Avdeef and W. P. Schaefer, *J. Am. Chem. Soc.*, in press.

(8) (a) G. A. Rodley and W. T. Robinson, *Nature (London)*, **235**, 438 (1972); (b) W. T. Robinson, Paper I5, American Crystallographic Association Winter Meeting, Gainesville, Fla., Jan 1973.

(9) M. Calligaris, C. Nardin, L. Randaccio, and C. Tauzher, *Inorg. Nucl. Chem. Lett.*, **9**, 419 (1973).
(10) B. C. Wang and W. P. Schaefer, *Science*, **166**, 1404 (1969).
(11) M. Calligaris, G. Nardin, L. Randaccio, and A. Ripamonti, *J. Chem. Soc. A*, 1069 (1970).
(12) L. A. Lindblom, W. P. Schaefer, and R. E. Marsh, *Acta Crystallogr., Sect. B*, **27**, 1461 (1971).
(13) No assumption about the formal oxidation states of either the cobalt atoms or the dioxygen ligand is implied by the name.
(14) W. P. Schaefer and R. E. Marsh, *Acta Crystallogr., Sect. B*, **25**, 1675 (1969).
(15) With the exception of C. K. Johnson's ORTEP program, the computer programs used were from Caltech's CRYM system: D. J. Duchamp, Abstacts, American Crystallographic Association Annual Meeting, Bozeman, Mont., 1964, Paper B14.
(16) S. W. Peterson and H. A. Levy, *Acta Crystallogr.*, **10**, 70 (1957).
(17) F. L. Hirshfeld and D. Rabinovich *Acta Crystallogr., Sect. A*, **29**, 510 (1973).
(18) (a) The function minimized was $S = \sum w(F_o^2 - F_c^2)^2$, where F_o^2 and F_c^2 are the observed and calculated structure factor square amplitudes and the weights w are taken as $1/\sigma^2(F_o^2)$. Neutral atom scattering factors were used for all the atoms.[18b,c] The real component of anomalous dispersion for cobalt atoms was included (interpolated as −2.19 electrons using Cromer's compilations[18d]). (b) "International Tables for X-Ray Crystallography", Vol. III, Kynoch Press, Birmingham, England, 1968, p 204. (c) R. F. Stewart, E. R. Davidson, and W. T. Simpson, *J. Chem. Phys.*, **42**, 3175 (1965). (d) D. T. Cromer, *Acta Crystallogr.*, **18**, 17 (1965).
(19) One block contained the coordinates while the thermal parameters along with the scale factor were divided between two other blocks in the 505-parameter refinement. The parameters of the solvent atoms were generally kept fixed during the main refinements. The total number of parameters, including the dependent ones, was 814.
(20) Two particularly troublesome reflections were the intense F_{002} and F_{020}. In the two- and three-orientation solvent models, the former was calculated some 50–100 electrons too high, while the latter was calculated about 80 electrons too low. This trend, also present in many other strong reflections, could be interpreted to mean that the solvent region was electron density deficient, since the two reflections above are proportional to cos $4\pi z$ and cos $4\pi y$ and the solvent molecule has the coordinate ranges $y = 0.43 \pm 0.06$ and $z = 0.26 \pm 0.04$. Since the z coordinate of one of the cobalt atoms is 0.52, the solvent region deficiency may have been compensated by the distortion of the cobalt thermal parameters. The sum of this and other smaller effects apparently resulted in the drastically distorted structure referred to as model A.
(21) The population factors were determined by comparing the magnitudes of the residual density peaks in the difference map, guided by the assumption that the thermal parameters of the two solvent molecules were approximately the same. The bond distances and angles were loosely constrained to be the expected ideal values.
(22) S. C. Abrahams and E. T. Keve, *Acta Crystallogr., Sect. A*, **27**, 157 (1971).
(23) A. Avdeef and W. P. Schaefer, to be submitted for publication.
(24) Supplementary material.
(25) (a) The agreement factors used in Table II are based on deviations of F^2 from the corresponding weighted means of groups of duplicated reflections. The individual-octant factors are defined as $R^i = \sum_n^{N_i}|\Delta_{ni}|/\sum \bar{F}_n^2$, $R_w^i = [(\sum \sigma_{ni}^2/\sigma_{ni}^2)/(\sum \bar{F}_n^4/\sigma_{ni}^2)]^{1/2}$, and the goodness of fit, $GOF^i = [N_i^{-1}\sum \Delta_{ni}^2/\sigma^2(\Delta_{ni})]^{1/2}$, where $\Delta_{ni} = F_{ni}^2 - \bar{F}_n^2$, $\sigma^2(\Delta_{ni}) = \sigma_{ni}^2 - 1/\sum_m(1/\sigma_{nm}^2)$, $\bar{F}_n^2$ is the nth weighted mean (interoctant) structure factor square amplitude, and N_i is the number of reflections in the ith octant which have duplicates in other octants. The overall (mean) agreement indices are defined as $R = \sum_n^N\sum_m^{M_n}|\Delta_{nm}|/\sum\sum F_{nm}^2$, $R_w = [(\sum\sum \Delta_{nm}^2/\sigma_{nm}^2)/(\sum\sum F_{nm}^4/\sigma_{nm}^2)]^{1/2}$, and $GOF = [N^{-1}\sum_n(M_n - 1)^{-1}\sum_m \Delta_{nm}^2/\sigma_{nm}^2]^{1/2}$, where N is the number of duplicate sets and M_n is the number of reflections in the nth set of duplicates. (b) The agreement factors (cf. ref 18a) reported for the model refinement are goodness of fit, $GOF = [S/(N_o - N_p)]^{1/2}$, where $N_o = 5314$ reflections and $N_p = 543$ independent parameters, $R_F = \sum||F_o| - |F_c||/\sum|F_o|$, $R_{wF} = [(\sum wF_o^2(|F_o| - |F_c|)^2)/(\sum wF_o^4)]^{1/2}$, and $R_{wF^2} = [S/\sum wF_o^4]^{1/2}$.
(26) Since a satisfactory weighting scheme was obtained from the merging of duplicate reflections, it did not seem justifiable to change the weighting scheme as a result of biases which were probably model based rather than data based.
(27) L. Pauling, "The Nature of the Chemical Bond", 3rd ed, Cornell University Press, Ithaca, N.Y., 1960, pp 351–352.
(28) The estimated standard deviations are based on isotropic coordinate errors and thus do not incorporate correlation effects.
(29) W. C. Hamilton, "Statistics in Physical Sciences", Ronald Press, New York, N.Y., 1964, Chapter 3.
(30) F. R. Fronczek, W. P. Schaefer, and R. E. Marsh, *Inorg. Chem.*, **14**, 611 (1975).
(31) F. R. Fronczek and W. P. Schaefer, *Inorg. Chim. Acta.* **9**, 143 (1974).
(32) R. E. Marsh and W. P. Schaefer, *Acta. Crystallogr., Sect. B*, **24**, 246 (1968).
(33) W. P. Schaefer and R. E. Marsh, *J. Am. Chem. Soc.*, **88**, 178 (1966); *Acta Crystallogr.*, **21**, 735 (1966).
(34) W. P. Schaefer, *Inorg. Chem.*, **7**, 725 (1968).
(35) F. R. Fronczek, W. P. Schaefer, and R. E. Marsh, *Acta Crystallogr., Sect B*, **30**, 117 (1974).
(36) J. R. Fritch, G. G. Christoph, and W. P. Schaefer, *Inorg. Chem.*, **12**, 2170 (1973).
(37) T. Shibahara, S. Koda, and M. Mori, *Bull. Chem. Soc. Jpn.*, **46**, 2070 (1973).
(38) U. Thewalt and R. E. Marsh, *J. Am. Chem. Soc.*, **89**, 6364 (1967); *Inorg. Chem.*, **11**, 351 (1972).
(39) G. G. Christoph, R. E. Marsh, and W. P. Schaefer, *Inorg. Chem.*, **8**, 291 (1969).
(40) C. Floriani and F. Calderazzo, *J. Chem. Soc. A*, 946 (1969).
(41) M. Calligaris, G. Nardin, and L. Randaccio, *Coord. Chem. Rev.*, **7**, 385 (1972).
(42) The first value in the brackets refers to the internally determined[43] estimated standard deviation in the least significant digit, while the second value refers to the externally determined error.
(43) W. C. Hamilton and S. C. Abrahams, *Acta Crystallogr., Sect. A*, **26**, 18 (1970).
(44) W. R. Scheidt, J. A. Cunningham, and J. L. Hoard, *J. Am. Chem. Soc.*, **95**, 8289 (1973).
(45) W. R. Scheidt, *J. Am. Chem. Soc.*, **96**, 84 (1974).
(46) V. Schomaker and K. N. Trueblood, *Acta Crystallogr., Sect. B*, **24**, 63 (1968).
(47) W. C. Hamilton and J. A. Ibers, "Hydrogen Bonding in Solids", W. A. Benjamin, New York, N.Y., 1968, p 16.
(48) Oxygen loss accounts for only 3.5% of the weight of the dimer. Yet the first observed weight loss in the thermogram is 17%, followed by an additional loss of 8% under 140 °C. The weight loss associated with the oxygen, the solvent, and one of the coordinated piperidine molecules is 20% and may explain the first observed loss. The loss of the other piperidine accounts for an additional 9%.

Contribution from the "Laboratoire de Chimie du Solide du CNRS", Université de Bordeaux I, 33405 Talence, France

Crystal Structure of Sodium Lanthanum Orthovanadate, $Na_3La(VO_4)_2$

M. VLASSE,* R. SALMON, and C. PARENT

Received December 2, 1975 AIC508670

The crystal structure of sodium lanthanum orthovanadate has been determined and refined by full-matrix least-squares methods using automatic diffractometer data to a residual $R = 0.081$. The space group is $Pbc2_1$ ($Pca2_1$) with $a = 5.582$ (2) Å, $b = 14.240$ (8) Å, and $c = 19.420$ (9) Å. The structure is made up of isolated VO_4 tetrahedra and of sodium and lanthanum atoms arranged in an ordered way. A description of the structure from a topological viewpoint has been given.

Introduction

Rare earth orthovanadates of formula $LnVO_4$ crystallize with the tetragonal zircon-type structure,[1,2] with the exception of $LaVO_4$ which has a monazite-type structure. They make up a unique series for the study of the relationships between structure and physical properties.

Since some of these compounds have interesting optical properties which seem to be related to the position of the Ln^{3+}